PV Based Three-Level NPC Shunt Active Power Filter with Extended Reference Current Generation Method

M. Vijayakumar
Department of Electrical and Electronics Engineering, K.S.R College of Engineering, Tiruchengode-637215, Tamilnadu, India
Email: mvijayksrce@gmail.com

S. Vijayan
Surya Engineering College, Erode-638107, Tamilnadu, India

***Abstract*—This paper proposes an extended reference current calculation method for the PV based three-level neutral point clamped (NPC) shunt active power filter (SAPF). Shunt active power filter demands a source of energy for compensating the current based distortions, which utilizes the photovoltaic array with DC-DC boost converter as a source of DC power. The shunt connected inverter controls the DC link voltage as well as the active and reactive power transferred between the renewable energy sources to grid with improved power quality. The proposed controller is based on the use of high selectivity filter (HSF) for reference current generations. In addition the fuzzy logic controller is implemented for better current control accuracy of shunt active filter. The main benefits of the proposed system are that it will provide uninterrupted compensation for the whole day and compensate the voltage interruption. This system utilizes the renewable energy and accordingly saves the energy, shares the load and provides uninterruptable power supply to critical/sensitive load, through the photovoltaic (PV) array/battery bank during the day and night. A simulation of the proposed topology has been carried out in the MATLAB/Simulink environment and the results are presented. Experimental studies are carried out to confirm the effectiveness of the proposed configuration.**

***Index Terms*—photovoltaic systems, DC-DC power converters, multi level NPC voltage source inverter, fuzzy control, total harmonic distortion**

I. Introduction

With the proliferation of power electronic converters are ever increasing in the processing of electrical energy in industrial applications like as adjustable-speed motor drives, electronic power supplies, direct current motor drives, battery chargers, etc. These devices are non-linear loads which draw nonlinear currents from the source and degraded the power quality in the power distribution network [1]. The severe power quality problems occurred in the distribution feeders are such as flicker, resonance and interference with electronic equipment, losses and heating in transmission lines, vibrations and noise in motors, malfunction and failures of metering/sensitive equipments. The several Custom power devices have been proposed for enhancing the power quality and reliability of electrical power. Initially, passive filters with tuned *LC* components have been mostly used to suppress harmonic current because of its low initial cost, simple in configuration and high efficiency [2], [3]. However, passive filters have many drawbacks such as fixed compensation, large size, parallel and series resonance with load, and utility impedances [4]. All the above mentioned drawbacks of passive filters can be overcome by using active power filters (APFs) [5], [6] for the harmonic elimination and reactive power compensation. Active power filters can be classified as a series or shunt according to their system configuration. The combination of series and shunt active power filters is called the unified power-quality compensator (UPQC). The SAPF is one of the most important corrective measures to solve source current harmonic problems [7].

The shunt active power filter is connected in parallel to the load and it generates the compensation current opposes to the load harmonic current. In recent years, multilevel NPC inverters are becoming increasingly popular in the active power filter application environment. This is due to the advantages obtained from these topologies, together with the low harmonic distortion of the voltage and current generated, the size of required filter elements are small, the higher efficiency of the system, the low *dv/dt*, the reduced common-mode voltages and less electromagnetic interference [8]. The performances of active filter topologies mainly depend on the reference current generation method, since any inaccuracy in the reference currents yields to incorrect compensation [9]. The various methods have been used to determine the reference current of the SAPF in the literature [10], can be categorized in frequency domain or time domain methods. The time domain methods require lesser computations compared to the frequency domain methods. One of the most commonly used methods is

Manuscript received May 14, 2014; revised December 10, 2014.

doi: 10.12720/ijoee.2.4.258-267

based on the conventional instantaneous reactive power theory or *p-q* theory [11]. However, the identification of the harmonic components with the *p-q* theory mainly depends on the quality of the voltage of the electrical power system. The SAPF schemes based on the *p-q* theory thus need the voltage components and this is conventionally done with a Phase Locked Loop (PLL) system [12]. But, this theory requires a number of transformations. However, these transformations, mostly consider the electrical system in balanced conditions which is not the real condition of electric networks. To overcome this problem, the proposed control strategy used is based on a modified version of *p-q* theory using two HSFs to extract the fundamental component directly from electrical signals (voltage and current) in α - β reference frame. In this method, the HSF has been used instead of classical harmonic extraction based on high pass filters (HPF) or low pass filters (LPF). After the efficient extraction of the reference current, an appropriate SAPF currents controller is used to maintain the active power filter currents at the imposed reference value [13], [14].

Various control approaches, such as the PI, PID, sliding-mode controllers, etc., are used by many authors in several works. However, the PI controller requires a specific linear mathematical model, which is complicated to obtain and may not give acceptable performance under different conditions such as parameter variations, unbalanced or distorted AC voltages, etc.

The fuzzy logic controllers have advantages over the PI controller such as: it does not need a precise mathematical model; it can work with imprecise inputs, it can handle nonlinearity and it is more robust than the PI controller [15], [16]. This paper extends the use of the proposed HSF within the SAPF based on a three-level inverter for a three-phase distribution system under the unbalanced conditions.

The main objectives of this paper are to maintain the DC link voltage of the three level neutral point clamped parallel connected inverter to provide uninterrupted compensation, utilizes the renewable energy, shares the load and provides the uninterruptable power supply to critical/sensitive load. The PV array is used to drive the High step-up DC-DC boost converter to step-up the voltage and maintain the DC-link voltage as constant. The PV array is connected to the boost converter in day time for continuous compensation and shares the load to the distribution system. During the night time, the battery will act as a DC source for the boost converter. This power only is used for compensation. When the compensation is not required for the system or excess power generated from the PV array, it charges the battery. The proposed system also eliminates the requirement of UPS and stabilizers for the individual equipments. In order to achieve the optimal utilization of PV system, a low step-up DC–DC converter associated with a function called maximum power point tracking (MPPT) is introduced between the PV array and battery. The simulation and experimental results are presented to validate the proposed method.

This paper presents the topology used and the entire scheme of operation of PV based three-level NPC shunt active power filter with the proposed control scheme. The proposed system has been implemented in hardware and its results were presented.

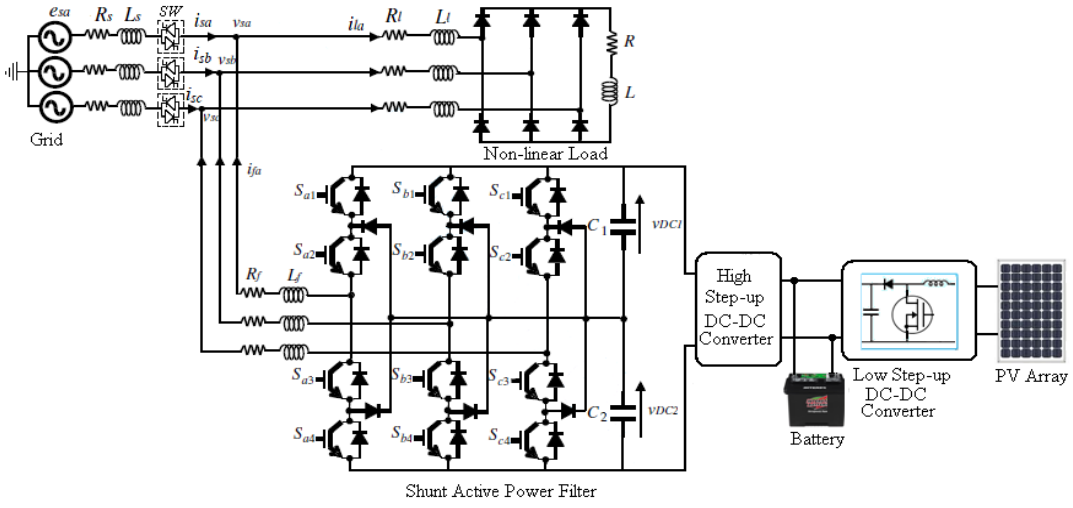

Figure 1. PV based neutral point clamped shunt active power filter configuration

II. Design of Three Level NPC Shunt Active Power Filter

The current harmonics elimination is achieved in the shunt active power filter by the injection of equal but opposite phase of the harmonic components of the nonlinear load current at the point of common coupling (PCC), accordingly it makes the source current in phase with the source voltage.

The proposed PV based shunt active power filter configuration is shown in Fig. 1 [10]. For three-level NPC inverter, each leg is constituted by four controllable switches (Sx_1-Sx_4), where *x* is specified phase (*a*, *b*, or *c*), with two clamping diodes. If we consider that two capacitor voltages v_{DC1} and v_{DC2} in the DC link are equal, three voltage levels (0, $v_{DC}/2$ and $-v_{DC}/2$) are generated on the AC terminal output of the proposed inverter. The

three states available with a single leg are shown in Table I. v_{fx} is the voltage between phase and fictive midpoint of the DC link. The SAPF is connected in parallel with a nonlinear load to produce reactive and harmonic currents opposed to those of the nonlinear loads to cancel the harmonic currents.

TABLE I. SWITCHING STATES OF 3 LEVEL NPC INVERTER

C_x	S_{x1}	S_{x2}	S_{x3}	S_{x4}	v_{fx}
1	1	1	0	0	$v_{DC}/2$
0	0	1	1	0	0
-1	0	0	1	1	$-v_{DC}/2$

It is assumed that the upper-leg and lower-leg capacitor voltages are identical, with the value $v_{DC}/2$ each. In this case, the phase-to-midpoint voltage of each phase can be defined:

$$v_{fx} = C_x v_{DC} / 2 \tag{1}$$

where x is the phase index, x=a, b, c; C_x is the state variable, C_x=1, 0, -1 and corresponding to the three-levels are $v_{DC}/2$, 0 and $-v_{DC}/2$.

Then, the phase-to-neutral voltage of the inverter given as:

$$v_{fa} = \frac{v_{DC}}{3}\left(C_a - \frac{C_b}{2} - \frac{C_c}{2}\right) \tag{2}$$

$$v_{fb} = \frac{v_{DC}}{3}\left(C_b - \frac{C_a}{2} - \frac{C_c}{2}\right) \tag{3}$$

$$v_{fc} = \frac{v_{DC}}{3}\left(C_c - \frac{C_a}{2} - \frac{C_b}{2}\right) \tag{4}$$

The proposed PV-SAPF operation has been divided into three modes of operation. The modes are (i) Inverter mode (ii) Compensator mode (iii) UPS mode.

i) Inverter mode: In this mode the operation starts working during the day time or solar irradiation available. During this period the proposed PV-SAPF is utilized to operate as a harmonic and reactive power compensator and shares the common load. The excessive power of the PV array charges the battery simultaneously.

ii) Compensator mode: When no active power is gained from the PV array, the system is utilized only to compensate the voltage and current based distortions and reactive power. The battery connected DC-DC boost converter manages the DC-link to provide continuity of compensation effectively.

iii) UPS mode: During the voltage interruption period, the PV-SAPF provides the uninterruptable power supply to critical/sensitive load, through the PV array and battery bank during day and night time respectively.

The grid power supply source is disconnected through the semiconductor switches (*SW*), when an occasional power interruption occurs in the incoming power supply.

III. MODELLING OF PHOTOVOLTAIC ARRAY

The PV array is the whole power generating unit, containing a number of solar panels to convert sunlight into electricity. The developments of efficient solar panels with MPPT algorithm have increased the usage of solar panels as an alternative source of renewable energy conversion. In the proposed system, PV array with DC-DC boost converter joined with a function called MPPT is incorporated to work as a DC voltage source for the shunt inverter. The electrical system powered by the PV array requires DC-DC converter because of the varying nature of the generated solar powered energy, caused by sudden changes in weather conditions, which modify the solar irradiation level along with cell operating temperature. The equivalent circuit model of photovoltaic array with DC-DC boost converter is shown in Fig. 2 [17].

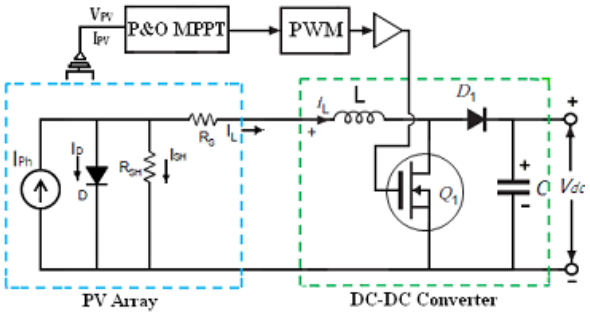

Figure 2. Equivalent circuit model of photovoltaic array with DC-DC boost converter

The PV array model is developed by the basic equations of photovoltaic cells, including the effects of temperature changes and solar irradiation level [18].

The output voltage of the PV cell is a function of photo current that is normally determined by load current depending on the solar irradiation level. The PV cell output voltage is expressed as

$$V_c = \frac{AkT_c}{e}\ln\left(\frac{I_{ph} + I_0 - I_c}{I_0}\right) - R_s I_c \tag{5}$$

$$V_{PV} = V_C \times N_s \tag{6}$$

$$I_c = \frac{I_{PV}}{N_P} \tag{7}$$

where, e is the charge the of electron $(1.602 \times 10^{-19} c)$, V_c is the output voltage of PV cell in volts, A is curve fitting factor (0.001), I_{Ph} is the photo current in A, I_0 is the reverse saturation current of diode, k is Boltzmann constant $(1.38 \times 10^{-23} J/^0 k)$, T_c is the operating temperature of the reference cell (25^0c), I_c is the cell output current in Ampere, R_s is the cell internal resistance (0.001Ω), V_{pv} is the output voltage of PV array, I_{PV} is the output current of the PV array, N_s is the number of series cell and N_p is the number of parallel cells.

The design parameters I_{ph}, I_o, R_s and T_c are determined from the data sheet and I-V characteristics of the PV

array. The curve fitting factor A is used to adjust I-V characteristics of the cell to the actual characteristics obtained by the testing.

The low step-up DC-DC converter comprises of a high speed MOSFET switch, inductor, diode and capacitor [19], [20]. The output voltage can be controlled by varying the switching duty cycle (D) of the switch Q_1. When the Q_1 is turned on using a pulse width modulation (PWM) generator, current starting flows through L and Q_1. The energy is stored in the inductor (L), the load current is supplied by the charge in capacitor C.

$$V_L = L_s \frac{di_s}{dt} \tag{8}$$

$$V_{in} = V_L \tag{9}$$

When the switch Q_1 is turned off, the inductor voltage adds to the source voltage and current due to this boosted voltage now flows from the source through inductor L, diode and the load, which recharges the capacitor C. The output voltage V_{out} during T_{off} can be expressed as,

$$V_{out} = V_{in} + L_s \frac{di_s}{dt} \tag{10}$$

The average output voltage of the converter is illustrated in the equation

$$V_{out} = \frac{V_{in}}{1 - D} \tag{11}$$

where, D is the duty Cycle, T_{on} is on time, T_{off} is off time and i_s is the current flowing through the inductor L_s and V_{in} is the input voltage.

IV. Maximum Power Point Tracking Method

In the renewable energy systems the solar power derived from the PV array is the main power source, and the battery bank serves as the backup power source. The renewable energy system to provide power for the compensation and load by PV panels as far as possible, and when solar power becomes excessive or insufficient, battery power provides the necessary power buffer as a storage or backup power source. In practice, MPPT for the PV power system is applied to collect power from the PV panels, and a DC-DC boost converter. In this paper, the Perturb & Observe algorithm [21] is chosen for MPPT controller implementation, as shown in Fig. 3.

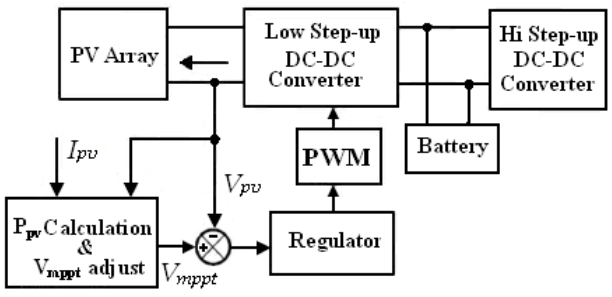

Figure 3. MPPT control system

V. High Step-Up DC-DC Converter

In the proposed configuration the output voltage level of the low step-up DC-DC converter/batteries are low. Accordingly, it is not enough to supply the required DC voltage to the DC link to compensate the voltage and current based distortions and voltage interruption through the parallel connected voltage source inverter. The high step up DC-DC converter is used to step-up the low DC voltage into high DC voltage (520V). Fig. 4 shows the circuit diagram of a high step up DC-DC converter [22]. The working principle of this converter is that when the switch S is turned on, the coupled inductor induces voltage on the secondary side and magnetic inductor L_m is charged by input voltage V_{in}. The induced voltage in the secondary makes V_{in}, V_{c1}, V_{c2} and V_{c3} to release energy to the converter output in the series. When the switch S is turned off, the energy stored in the magnetic inductor L_m is released via the secondary side of coupled inductor to charge the capacitors C_2 and C_3 in parallel.

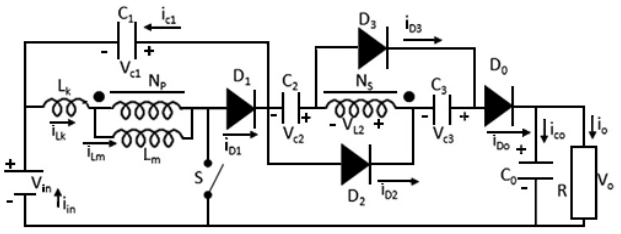

Figure 4. Circuit diagram of high step up DC-DC converter

The proposed converter operation can be divided into five modes of operation in one switching period.

The output voltage of high step-up DC-DC converter is given as

$$V_o = V_{in} + V_{C1} + V_{C2} + v^{I}_{L2} + V_{C3} \tag{13}$$

where, V_{c1}, V_{c2} and V_{c3} are the voltages in volts across the capacitor $C1$, $C2$ and $C3$ respectively. v^{I}_{L2} is the voltage across the secondary of the coupled inductor (Ns) in mode II.

The voltages across the capacitors $C1$, $C2$, and coupled inductor (N_S) are obtained as follows:

$$V_{C1} = \frac{D}{1 - D} V_{in} \frac{(1 + k) + (1 - k)n}{2} \tag{14}$$

$$V_{C2} = V_{C3} = \frac{nDk}{1 - D} V_{in} \tag{15}$$

$$v^{I}_{L2} = kV_{in} \tag{16}$$

where, k is the coupling coefficient, n is the coupled inductor turns ratio (N_s/N_p) and D is the duty cycle. The main role of this converter is to maintain the constant voltage across the DC link of shunt inverter. The simple control structure with PI controller is implemented for the high step-up DC-DC converter to maintain the constant DC link voltage as shown in Fig. 5. The control block consists of LPF, PI controller, sawtooth wave generator, comparator and relational operator [23], [24]. The output

of the PI controller gives the control signal required to the relational operator to generate the required duty cycle by comparing the processed error signal and saw tooth wave.

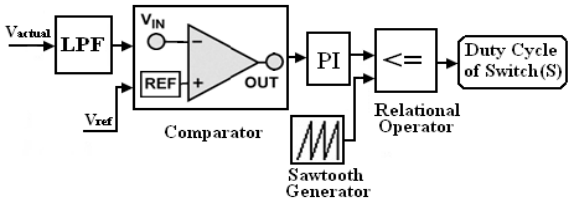

Figure 5. Controller for high step up DC-DC converter

VI. Proposed Control Scheme

The proposed control structure of the three-level shunt active power filter comprises of four basic elements: To identify the harmonic current and form a synchronized reference, the generation of the gate signal of the active power filter, Provide closed-loop control to force the filter current to follow the reference and To regulate the DC capacitor voltage of SAPF to maintain the DC voltage at a constant value.

A. Calculation of Reference Currents

In order to control the SAPF to supply a current that is equal to the amplitude and opposite in direction of the load current, a reference current was required. In this control scheme the reference current signal is derived from the measured quantities by the utilization of the instantaneous reactive power theory associated with 2 HSFs.

The key steps of this approach are summarized in the simplified block diagram shown in Fig. 6. The reference currents are identified by using a modified version of the instantaneous active and reactive power theory. We used HSF in place of classical harmonic extraction based on HPF or LPF. The HSF is focused on to extract the fundamental component directly from unbalanced electrical signals (voltage or current) in α - β reference frame.

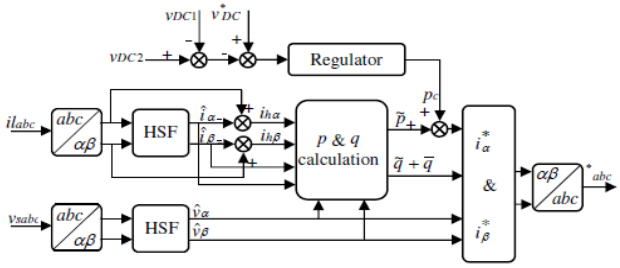

Figure 6. Block diagram of proposed controller

Based on the instantaneous reactive power theory, the system voltage and the load current are transformed from *a-b-c* coordinates into α-β coordinates using the transformations (17) and (18) [25], [26]:

$$\begin{bmatrix} v\alpha \\ v\beta \end{bmatrix} = \sqrt{\frac{2}{3}} \begin{bmatrix} 1 & -\frac{1}{2} & -\frac{1}{2} \\ 0 & \frac{\sqrt{3}}{2} & -\frac{\sqrt{3}}{2} \end{bmatrix} \begin{bmatrix} vsa \\ vsb \\ vsc \end{bmatrix} \quad (17)$$

$$\begin{bmatrix} i\alpha \\ i\beta \end{bmatrix} = \sqrt{\frac{2}{3}} \begin{bmatrix} 1 & -\frac{1}{2} & -\frac{1}{2} \\ 0 & \frac{\sqrt{3}}{2} & -\frac{\sqrt{3}}{2} \end{bmatrix} \begin{bmatrix} ila \\ ilb \\ ilc \end{bmatrix} \quad (18)$$

The alternating components of the instantaneous real and imaginary power are identified by:

$$\begin{bmatrix} \tilde{p} \\ \tilde{q} \end{bmatrix} = \begin{bmatrix} \hat{v}\alpha & \hat{v}\beta \\ -\hat{v}\beta & \hat{v}\alpha \end{bmatrix} \begin{bmatrix} ih\alpha \\ ih\beta \end{bmatrix} \quad (19)$$

A fundamental component of the instantaneous imaginary power is given as follows

$$\overline{q} = \hat{v}\beta\, \tilde{i}\alpha - \hat{v}\alpha\, \tilde{i}\beta \quad (20)$$

After adding the active power required for regulating DC bus voltage, p_c, to the alternative component of the instantaneous real power, $\tilde{p}$, the current references in the α-β reference frame are calculated:

$$i^*\alpha = \frac{\hat{v}\alpha}{\hat{v}^2\alpha + \hat{v}^2\beta}\left(\tilde{p} + pc\right) - \frac{\hat{v}\beta}{\hat{v}^2\alpha + \hat{v}^2\beta}\left(\tilde{q} + \overline{q}\right) \quad (21)$$

$$i^*\beta = \frac{\hat{v}\beta}{\hat{v}^2\alpha + \hat{v}^2\beta}\left(\tilde{p} + pc\right) - \frac{\hat{v}\alpha}{\hat{v}^2\alpha + \hat{v}^2\beta}\left(\tilde{q} + \overline{q}\right) \quad (22)$$

In order to acquire the reference compensation currents in *a-b-c* co-ordinates, the inverse of the transformation given in expression (17) is used as follows:

$$\begin{bmatrix} i^*a \\ i^*b \\ i^*c \end{bmatrix} = \sqrt{\frac{2}{3}} \begin{bmatrix} 1 & 0 \\ -\frac{1}{2} & \frac{\sqrt{3}}{2} \\ -\frac{1}{2} & -\frac{\sqrt{3}}{2} \end{bmatrix} \begin{bmatrix} i^*\alpha \\ i^*\beta \end{bmatrix} \quad (23)$$

B. Identification of the Harmonic Component Using HSF:

The HSFs are used for the harmonic extraction instead of classical extraction filters such as a high pass filter or low pass filters.

Hong-sock Song [27] had presented that the integration in the synchronous reference frame is defined by:

$$Vxy(t) = e^{j\omega t} \int e^{-j\omega t} Uxy(t)dt \quad (24)$$

where, *Uxy* and *Vxy* are the instantaneous signals, respectively before and after integration in the synchronous reference frame. The equation (24) can be expressed by the following transfer function, after Laplace transformation:

$$H(s) = \frac{Vxy(s)}{Uxy(s)} = \frac{s + j\omega}{s^2 + \omega^2} \quad (25)$$

We introduced a constant K in the transfer function $H(s)$, to obtain a HSF with a cutoff frequency ωc. Therefore, the previous transfer function becomes:

$$H(s) = \frac{Vxy(s)}{Uxy(s)} = K\frac{(s+K)+j\omega c}{(s+K)^2+j\omega c^2} \quad (26)$$

By replacing $Vxy(s)$ by $X\alpha\beta(s)$ and $Uxy(s)$ by $\hat{X}_{\alpha\beta}(s)$, the following expressions can be obtained:

$$\hat{X}\alpha(s) = \frac{K(s+K)}{(s+K)^2+\omega c^2}X\alpha(s) - \frac{K\omega c}{(s+K)^2+\omega c^2}X\beta(s) \quad (27)$$

$$\hat{X}\beta(s) = -\frac{K\omega c}{(s+K)^2+\omega c^2}X\alpha(s) + \frac{K(s+K)}{(s+K)^2+\omega c^2}X\beta(s) \quad (28)$$

where, X can either be a current or a voltage. The equations (27) and (28) can be expressed as follows:

$$\hat{X}\alpha(s) = \frac{K}{s}\left[X\alpha(s)-\hat{X}\alpha(s)\right] - \frac{\omega c}{s}\hat{X}\beta(s) \quad (29)$$

$$\hat{X}\beta(s) = \frac{K}{s}\left[X\beta(s)-\hat{X}\beta(s)\right] + \frac{\omega c}{s}\hat{X}\alpha(s) \quad (30)$$

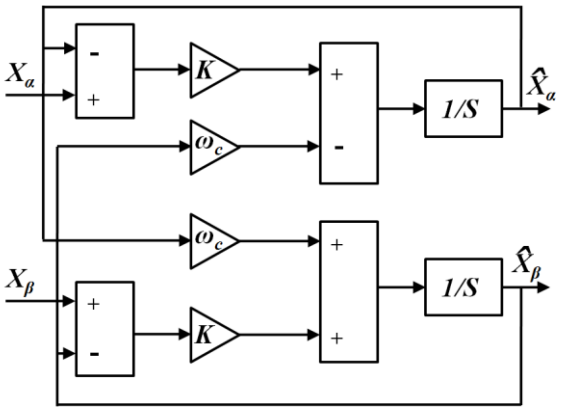

Figure 7. Block diagram of HSF

The block diagram of the HSF shows in Fig. 7 for extracting the fundamental component $\hat{X}\alpha\beta(s)$ from the signal $X\alpha\beta$ (s) in the α-β reference frame.

C. SAPF Gating Signals Generation

The performances of SAPF will depend essentially on the type of modulation and adopted current controller. The several modulation strategies have been proposed for multilevel converters in three-phase system. The modulation techniques are normally divided into two main categories. The first technique is based on hysteresis comparators, which is characterized by a very simple and easy to implement, moreover, it has the disadvantage of uncontrollable switching frequency. The next technique is PWM, which allows operating at a fixed switching frequency, such as for example sinusoidal PWM (SPWM) and space vector modulation (SVM).

In this proposed system, the carrier-based SPWM is used to generate the appropriate switching signals of the power switches, since it has the advantage of making significantly simpler the calculation process and due to their operation at fixed switching frequency [28], [29].

The switching SPWM pulses are generated by subtracting the filter currents (i_{fa}, i_{fb}, i_{fc}) with the reference currents (ia^*, ib^*, ic^*). The resulting error (e) ($e = i^* - i_f$) is sent to a fuzzy logic controller. Then the output signal of the fuzzy logic controller is compared with a two triangular carrier bipolar signal shown in Fig. 8 [30].

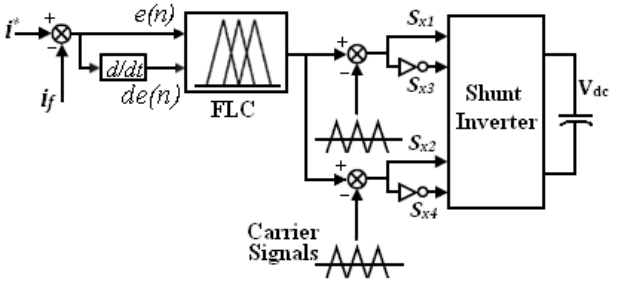

Figure 8. Fuzzy logic controller scheme

The comparison result is sent to the combinational logic circuit for the switching devices. Here, the gating signal generator has three inputs: $\Delta i_f = i^* - i_f$ (corresponding to Δi_{fa}, Δi_{fb} and Δi_{fc}), the first carrier-signal C_{s1}, and the second carrier-signal C_{s2}. Initially, we have to determine the intermediate signals T_1, T_2 and T_3 as follows:

- If $\Delta if \geq Cs_1$, then T_1=1, else T_1=0;
- If $\Delta if \geq Cs_2$, then T_2=0, else T_2=-1;
- $T_3 = T_1 + T_2$.

After that, we obtain the switching function of the two switches S_{x1} and S_{x2} of the upper leg x (x=a, b, c), the two other legs have switching signals delayed of 120° compared to the first one, and the lower half bridge contains the complementary switches.

D. Proposed Fuzzy Control Scheme

The main purpose of the AFLC structure is to reduce the control scheme complexity and, at the same time, to keep a high level of the dynamic performances and statics of the process, whose modeling is complicated or whose parameters are inaccessible. The current control loop is responsible for controlling the active power filter currents in the proposed control scheme circuit such that the current will try to be the same as the current reference. For this purpose, we are interested to control the active power filter current by a fuzzy controller as shown in Fig. 9. In our application, the fuzzy controller has two inputs: the difference between the injected current and the reference current is error (e) ($e = i^* - i_f$) and the derivation of the error (de) while the output is the command (cde).

We choose three fuzzy sets for each of the two inputs (e, de) with Gaussian membership functions, and five fuzzy sets for the output with triangular membership functions. For this, each linguistic variable (e, de, cde) is characterized by five terms of fuzzy subsets: Negative big (NB), Negative (N), zero (ZE), Positive (P), and Positive big (PB).

The fuzzy controller uses the following five simplified rules:

1. If (*e*) is zero (ZE), then (*cde*) is zero (ZE).
2. If (*e*) is positive (P), then *(cde)* is big positive (BP).
3. If (*e*) is negative (N), then (*cde*) is big negative (BN).
4. If (*e*) is zero (ZE) and *(de)* is positive (P), then *(cde)* is negative (N).
5. If (*e*) is zero (ZE) and *(de)* is negative (N), then *(cde)* is positive (P).

The inference engine output variables are converted into the crisp values in the defuzzification stage. Various defuzzification algorithms have been proposed in the literature. In this paper, the centroid defuzzification algorithm is used, in which the crisp value is calculated as the centre of gravity of the membership function 5.

VII. Simulation Results

In this paper, the proposed control scheme based on a modified version of p-q theory using a HSF for the PV based SAPF is evaluated using Matlab/Simulink software under unbalanced and distorted load-current and source-voltage conditions.

In the simulation studies, the results are specified before and after the operation of the PV based three-level SAPF system. The simulation study was conducted under three different conditions are balanced voltages with balanced loads, balanced voltages with unbalanced loads and unbalanced voltages with unbalanced loads. The comprehensive simulation results are presented below.

A. Balanced Voltages with Balanced Loads

Fig. 9 Shows the simulation results of load currents (i_{labc}) before compensation, active filter currents (i_{fabc}), source currents (i_{sabc}) after compensation, inverter output line voltage, and source phase voltage (v_{sa}) superimposed by the source current (i_{sa}) of the proposed system for the case of balanced condition. Fig. 9(e) shows the source current (i_{sa}) after the compensation, from this result examined that the source current is in phase with source voltage (v_{sa}) confirming that the compensation is being done correctly.

The harmonic analysis of the source current before and after compensation in phase "*a*" are shown in Fig. 10(a) and 10(b) respectively. Before compensation, the measured total harmonic distortion (THD) level of the source current in phase "*a*" was 25.65%; after compensation, the THD level of the source current is about 1.54%, which is well within the limit specified by IEEE Std. 519-1992.

Fig. 11 shows the PV array output voltage and high step-up DC-DC converter output voltage. A control circuit is incorporated with the proposed high step-up DC-DC converter to regulate the output voltage at 520V. The DC-link voltages, v_{DC1} and v_{DC2} must be maintained almost as a constant value within certain limits in order to provide energy to generate the required harmonic compensation current from the shunt active filter.

Fig. 12 shows the discharge characteristic of the battery for various current outputs. From the characteristics, it is observed that the bttery can feed 60A for 8 hours duration.

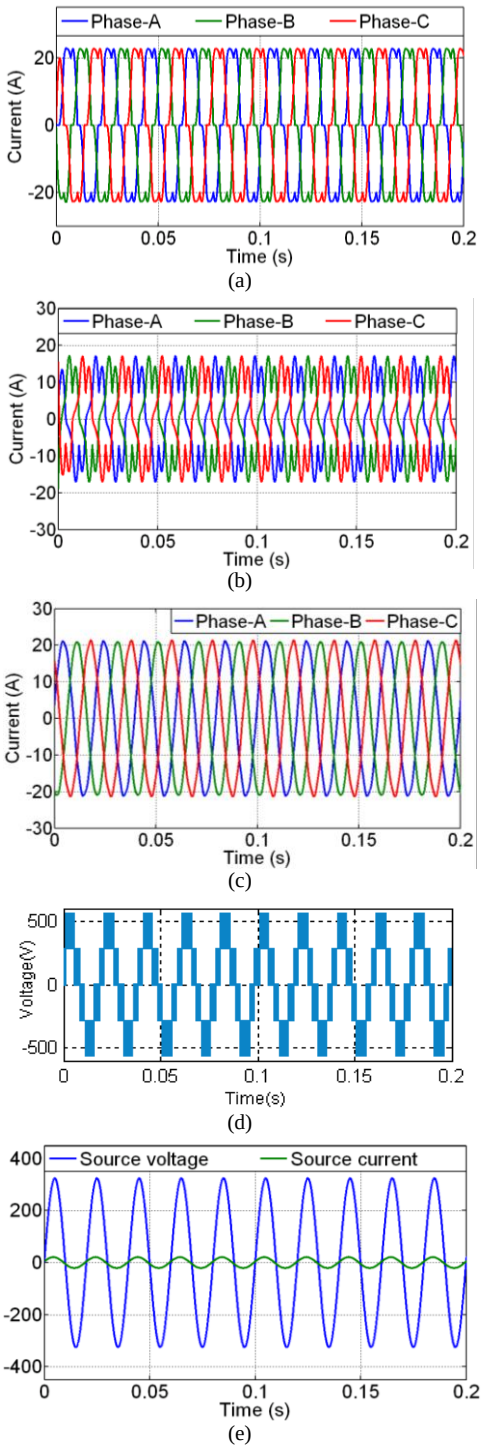

Figure 9. Simulation results under balanced voltages with balanced loads: (a) load currents (i_{labc}) (b) source currents (i_{sabc}) (c) active filter currents (i_{fabc}) (d) inverter output line voltage (e) source phase voltage (e_{sa}) superimposed by the source current (i_{sa}).

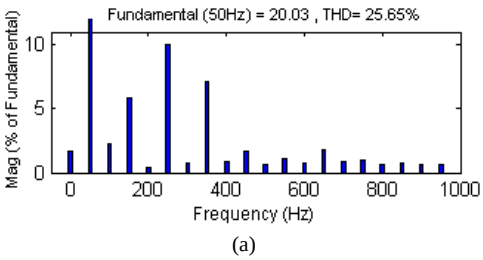

(a)

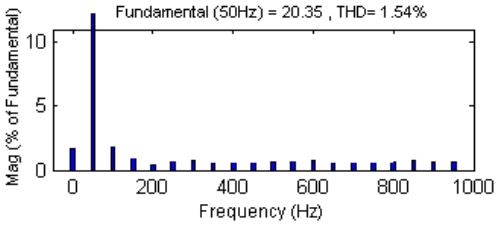

(b)

Figure 10. THD levels of source current (a) THD level of source current before compensation in phase 'a' (b) THD level of source current after compensation in phase 'a'

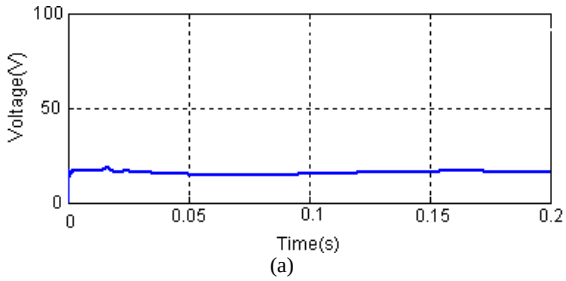

(a)

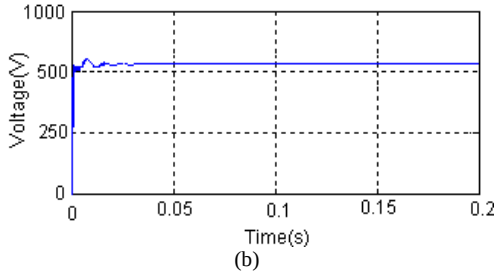

(b)

Figure 11. PV array output voltage and high step-up DC–DC converter output voltage

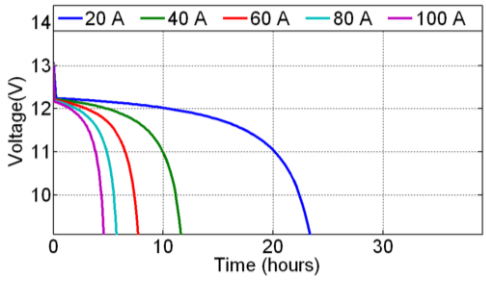

Figure 12. Discharge characteristics of the battery for various output currents

B. Balanced Voltages with Unbalanced Loads

In this case, the load currents are unbalanced by connecting a single phase diode rectifier connected between two phases. Fig. 13 Shows the simulation results of load currents (i_{labc}), source currents (i_{sabc}), active filter currents (i_{fabc}), and source voltage (e_{sa}) superimposed by the source current (i_{sa}). THD level of the three phase currents before installing the active power filter are 25.6%, 26.61% and 26.71% respectively. The harmonic spectrum of the source current in phase "*a*" after installing the active power filter with modified *p-q* theory is shown in Fig. 14. The THD level has reduced to 2.02%, 1.82% and 1.74% in phase "*a*", "*b*" and "*c*" respectively. In addition, the source current is in phase with the source voltage, so that the power factor is equal to one as shown in Fig. 13(d).

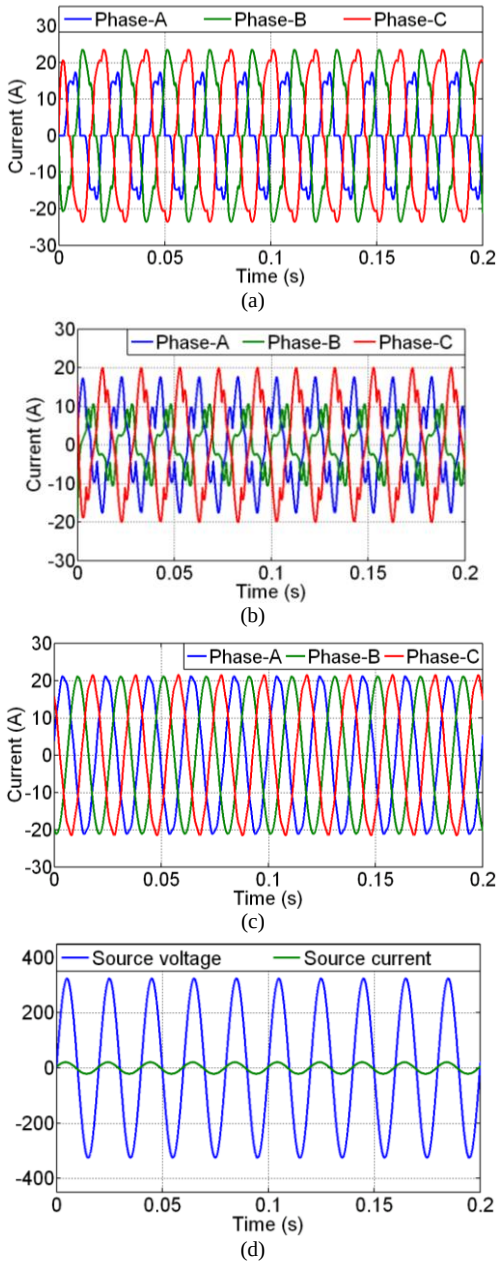

(a) (b) (c) (d)

Figure 13. Simulation results under balanced voltages with unbalanced loads: (a) load currents (i_{labc}) (b) source currents (i_{sabc}) (c) active filter currents (i_{fabc}) (d) source voltage (e_{sa}) and source current (i_{sa}).

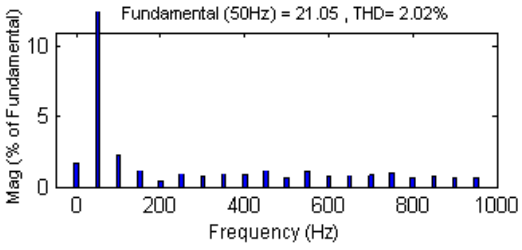

Figure 14. THD level of source current after compensation of phase '*a*'.

C. Unbalanced Voltages with Unbalanced Loads

For evaluating the performance of the SAPF under the unbalanced voltages with unbalanced loads, the previous unbalanced non-linear load is fed by unbalanced AC

voltages. The unbalanced source voltages (e_{sabc}), unbalanced load currents (i_{labc}), active filter currents (i_{fabc}), source currents (i_{sabc}) and source voltage (e_{sa}) superimposed by the source current (i_{sa}) are depicted in Fig. 15. The results shown in Fig. 15 confirm that the PV based SAPF system is able to improve the power quality. As shown in Fig. 15(c), it is evident that three phase source currents are balanced and sinusoidal after compensation, with power factor close to the unity, as can be observed in Fig. 16(e). The frequency analyses of the source current after compensation in phase "*a*" is shown in Fig. 16. The THD of the source currents before compensation are 22.53%, 26.11% and 30.64%; and are reduced to 2.12%, 1.86% and 1.82% after compensation respectively. Simulation results show that the proposed control strategy compensates harmonic components as well as most of the other unbalanced load current distortion in electric power systems with three-phase four-wire.

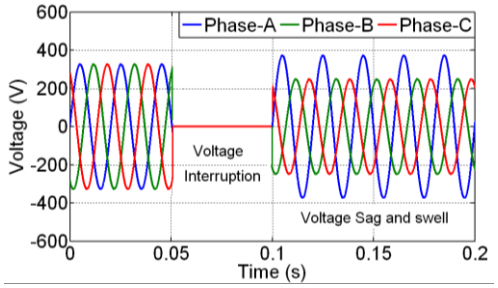

(a)

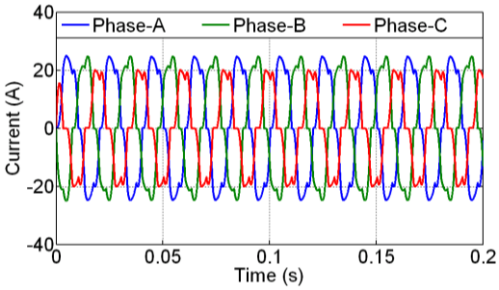

(b)

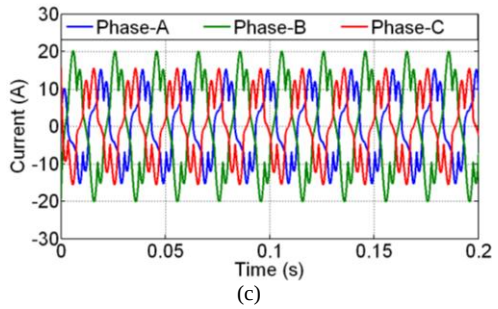

(c)

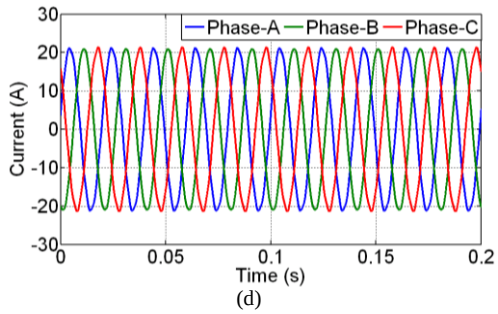

(d)

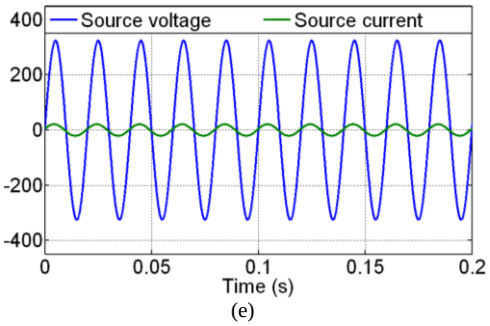

(e)

Figure 15. Simulation results under unbalanced voltages with unbalanced loads: (a) unbalanced source voltages (e_{sabc}) (b) load currents (i_{labc}) (c) active filter currents (i_{fabc}) (d) source currents (i_{sabc}) (e) source voltage (e_{sa}) and source current (i_{sa}).

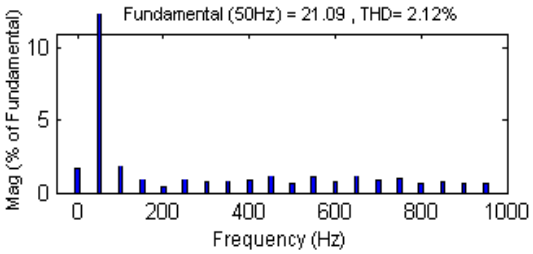

Figure 16. THD level of the source current after compensation in phase "*a*".

The THD level of the source currents for balanced/unbalanced voltage with unbalanced load conditions is very less about 1.93% in the proposed method when compared with the existing methods in which the THD levels are 2.5% and 4.3% as proposed by Abdusalam *et al* 2009 and Mehmet Ucar *et al* 2013 respectively [14], [31].

VIII. Conclusions

This paper investigates a new reference current generation approach based on a modified version of the *p-q* theory using a high selectivity filter. This approach is proposed in the PV based three level SAPF for current based compensation, reactive power and voltage interruption compensation at residence or small industry. A DC-DC converter with P&O MPPT algorithm is implemented to track the maximum power point of the PV array. Additionally, fuzzy logic controller is introduced for controlling compensation currents of the shunt active power filter. This novel PV- three level shunt active power filter is designed to reduce the energy consumption from the utility grid by sharing the common load, when the PV array generates required real power to meet the load demand. The added advantages of the system are: reducing the panel tariff and avoiding the use of UPS and power quality conditioner for the individual equipment at a residence, small industry and educational institution. The simulation and experimental results show that, when under balanced, unbalanced and non-linear load conditions, the proposed control scheme eliminates the impact of distortion and unbalance of the load current on the power system.

REFERENCES

[1] B. Singh, *et al.*, "A review of three-phase improved power quality AC-DC converters," *IEEE Trans. on Ind. Electron.*, vol. 51, no. 3, pp. 641-660, Jun. 2004.

[2] V. F. Corasaniti, M. B. Barbieri, P. L. Arnera, and M. I. Valla, "Hybrid power filter to enhance power quality in a medium-voltage distribution network," *IEEE Trans. on Ind. Electron.*, vol. 56, no. 8, pp. 2885-2893, Aug. 2009.

[3] S. Bhattacharya, D. M. Divan, and B. B. Banerjee, "Control and reduction of terminal voltage total harmonic distortion (THD) in a hybrid series active and parallel passive filter system," in *Proc. IEEE Power Electron. Specl. Conference*, Jun. 1993, pp. 779-786.

[4] F. Z. Peng, "Application issues of active power filters," *IEEE Ind. Appl. Mag.*, vol. 4, no. 5, pp. 21-30, 1998.

[5] H. Fujita and H. Akagi, "A practical approach to harmonic compensation in power systems-series connection of passive and active filters," *IEEE Trans. on Ind. Appl.*, vol. 27, no. 6, pp. 1020-1025, 1991.

[6] H. Akagi, "Control strategy and site selection of a shunt active filter for damping of harmonic propagation in power distribution systems," *IEEE Trans. on Power Delivery*, vol. 12, no. 1, pp. 354-362, Jan. 1997.

[7] B. Singh, K. Al-Haddad, and A. Chandra, "A review of active filters for power quality improvement," *IEEE Trans. Ind. Electron.*, vol. 46, no. 5, pp. 960-971, Oct. 1999.

[8] S. Ceballos, J. Pou, E. Robles, J. Zaragoza, and J. L. Martin, "Performance evaluation of fault-tolerant neutral point-clamped converters," *IEEE Trans. Ind. Electron.*, vol. 57, no. 8, pp. 2709-2718, Aug. 2010.

[9] K. Vardar, E. Akpinar, and T. Surgevil, "Evaluation of reference current extraction methods for DSP implementation in active power filters," *Elect. Power Syst. Res.*, vol. 79, pp. 1342-1352, 2009.

[10] N. Y. Dai, M. C. Wong, and Y. D. Han, "Application of a three-level NPC inverter as a three-phase four-wire power quality compensator by generalized 3 DSVM," *IEEE Trans. on Power Electron.*, vol. 21, no. 2, pp. 440-449, Mar. 2006.

[11] H. Akagi, Y. Kanazawa, and A. Nabae, "Instantaneous reactive power compensators comprising switching devices without energy storage components," *IEEE Trans. on Indl. Appl.*, vol. IA-20, no. 3, pp. 625-630, 1984.

[12] M. A. E. Alali, S. Saadate, Y. A. Chapuis, and F. Braun, "Advanced corrector with FPGA-based PLL to improve performance of series active filter compensating all voltage disturbances," in *Proc. European Conference on Power Electron. and Appl.*, Aug. 2001.

[13] S. Karimi, P. Poure, and S. Saadate, "High performances reference current generation for shunt active filter under distorted and unbalanced conditions," in *Proc. IEEE Power Electron. Specl. Conference*, Jun. 2008, pp. 195-201.

[14] M. Abdusalam, P. Poure, S. Karimi, and S. Saadate, "New digital reference current generation for shunt active power filter under distorted voltage conditions," *Elect. Power Syst. Res.*, vol. 79, pp. 759-765, 2009.

[15] A. Hamadi, K. Al-haddad, S. Rahmani, and H. Kanaan, "Comparison of fuzzy logic and proportional integral controller of voltage source active filter compensating current harmonics and power factor," in *Proc. IEEE Int. Conference Ind. Techn., IEEE*, 2004, vol. 2 , pp. 645-650.

[16] A. Dellaquila, A. Lecci, and V. G. Monopoli, "Fuzzy controlled active filter driven by an innovative current reference for cost reduction," in *Proc. IEEE Int. Symp. Ind. Electron.*, 2002, vol. 3, pp. 948-952.

[17] M. Vijayakumar and S. Vijayan, "Design and implementation of PV based three-phase four-wire series hybrid active power filter for power quality improvement," *Indian Academy of Sciences*, vol. 39, no. 4, pp. 859-877, 2014.

[18] H. Altas and A. M. Sharaf, "A photovoltaic array simulation model for MATLAB simulink GUI environment," in *Proc. ICCEP*, 2007, pp. 341-345.

[19] W. Jiang, Y. Zhou and J. Chen, "Modeling and simulation of boost converter in CCM and DCM," in *Proc. IEEE Conference*, 2009, pp. 288-291.

[20] N. Mazouz and A. Midoun "Control of a DC/DC converter by fuzzy controller for a solar pumping system," *Int. J Electr. Power Energy Syst.*, vol. 33, no. 10, pp. 1623-1630, 2011.

[21] T. Esram and P. L. Chapman, "Comparison of photovoltaic array maximum power point tracking techniques," *IEEE Trans. Energy Conv.*, vol. 22, no. 2, pp. 439-449, Jun. 2007.

[22] Y. P. Hsieh, J. F. Chen, T. J. Liang and L. S. Yang, "Novel high set-up DC-DC converter for distributed generation system," *IEEE Trans. Ind. Electron.*, vol. 60, no. 4, pp. 1473-1482, 2011.

[23] Y. H. Chang and K. W. Wu, "High-Conversion-Ratio switched capacitor DC-DC converter with bidirectional power flow," in *Proc. Multi Conference of Engineers and Computer Scientists*, 2011, vol. 2. pp. 1-6.

[24] M. Abdusalam, P. Poure, and S. Saadate, "Study and experimental validation of harmonic isolation based on high selectivity filter for three-phase active filter," in *Proc. IEEE Int. Symp. Ind. Electron.*, 2008, pp. 166-171.

[25] J. L. Afonso, M. J. S. Freitas, and J. S. Martins, "P-Q theory power components calculations," in *Proc. IEEE Int. Symp. Ind. Electron.*, 2003, vol. 1, pp. 385-390.

[26] M. C. Benhabib and S. Saadate, "New control approach for four-wire active power filter based on the use of synchronous reference frame," *Elect. Power Syst. Res.*, vol. 73, pp. 353-362, 2005.

[27] H.-S. Song, H.-G. Park, and K. Nam, "An instantaneous phase angle detection algorithm under unbalanced line voltage condition," in *Proc. IEEE Power Electron. Specl. Conference*, 1999, vol.1, pp. 533-537.

[28] J. Rodriguez, J. S. Lai, and F. Z. Peng, "Multilevel inverters: A survey of topologies, controls and applications," *IEEE Trans. on Ind. Electron.*, vol. 49, no.4, pp. 724-738, Aug. 2002.

[29] H. Zhang, S. J. Finney, A. Massoud, and B. W. Williams, "An SVM algorithm to balance the capacitor voltages of the three-level NPC active power filter," *IEEE Trans. on Power Electron.*, vol. 23, no. 6, pp. 2694-2702, Nov. 2008.

[30] H. Djeghloud, H. Benalla, and L. Louze, "A three-level shunt active power filter devoted to wind power applications," in *Proc. Int. Conference on Ecologic Vehicles and Renew. Energies*, 2007.

[31] M. Ucar and S. Ozdemir, "3-Phase 4-leg unified series-parallel active filter system with ultracapacitor energy storage for unbalanced voltage sag mitigation," *Int. J Electr. Power Energy Syst.*, vol. 49, pp. 149-159, 2013.

M. Vijayakumar received B.E. degree in Electrical and Electronics Engineering from the Bharathidasan University, Trichy, India in 1998. And he received the M.E. degree in Power Systems Engineering from the Anna University of Technology, Coimbatore in 2009. He is currently pursuing Ph.D. degree in Electrical Engineering, Anna University, Chennai. He is working as Associate professor at the department of Electrical and Electronics Engineering, K.S.R. College of Engineering, Tiruchengode-637215, Tamilnadu, India. His research interests are Power quality, FACTS, Harmonic Optimization Techniques and Grid connected renewable energy systems.

Dr. S. Vijayan received the B.E. degree from Madurai Kamaraj University, Tamilnadu, India in 1989 and the M.E. degree in Power System from Annamalai University, Chidambaram in 1993. He received Ph.D. in Electrical Engineering from Anna University, Chennai in 2008. He is currently Professor and Principal of Surya Engineering College, Erode, Tamilnadu. His research interests include Power Electronics and Drives, Renewable energy systems and power system optimization and smart grids.